EFFECT OF A FUNNEL-SHAPED RADIATION SHIELD ON THE CHARACTERISTICS OF A SILICON CZ FURNACE

KOJI HONDA AND NOBUYUKI IMAISHI
Institute of Advanced Material Study, Kyushu University, Kasuga 816
TAKAO TSUKADA AND MITUNORI HOZAWA
Institute for Chemical Reaction Science, Tohoku University, Sendai 980

Key Words: Crystal Growth, Silicon, Single Crystal, Radiation Heat Transfer, Thermal Stress, Finite Element Analysis, Czochralski Method

For the 6″ silicon CZ system, effects of a funnel-shaped radiation shield on the temperature profiles in the melt and crystal, the melt/crystal interface shape and also the distribution of the thermal stresses were investigated theoretically by the finite element analysis based on the conduction-dominated model.

It is found that a funnel-shaped radiation shield can make the melt/crystal interface less convex to the crystal (relatively flatter), providing a higher pull rate and smaller thermal stresses in the crystal compared with other radiation shield geometries, such as a doughnut (torus) shape. Also, the principal operating conditions in the CZ system, such as the crucible temperature, can be changed widely by selecting the emissivity and/or thickness of the shield.

Introduction

In the Czochralski (CZ) method for the growth of high-quality single crystals, it is important to control the crystal diameter, melt/crystal interface shape, thermal stresses and thermal history of the crystal. A high pulling rate and a reduction in electric power consumption are also required from the industrial point of view. These process-features are closely related to the heat transfer processes in the CZ system, and thus can be improved by an accurate knowledge of the heat transfer mechanism and by strict control of the temperature field in the furnace.

Recently, a number of theoretical studies[1-6,8-13,18] of the heat transfer processes during CZ crystal growth have been carried out in order to determine the processing conditions and system configurations for suitable CZ operations. For instance, Bornside *et al.*[1] suggested that the silicon CZ system can be modified by adding to or changing the geometries of a heat shield, and then the thermal stresses in the crystal can be reduced. Dupret *et al.*[7] investigated numerically the effect of the heat shield in the LEC furnace on the temperature and thermal stress fields in GaAs crystal. The heat shields addopted by these authors are set far above the rim of the crucible. In the previous works[15-17], we also computed the effects on silicon CZ crystal growth of a radiation shield that is set close to the melt surface, and concluded that the radiation shield can make the melt/crystal interface flatter, increase the pull rate, reduce power consumption and also reduce the thermal stresses in the crystal.

In some industrial CZ furnaces a funnel-shaped structure set close to the melt surface is effectively used to increase the desorption rate of SiO through its rectification of Ar gas flow, and also to increase the pulling rate. However, the effect of this structure on the radiative heat transfer in CZ system has not been studied quantatively.

In the present work we computed the temperature and thermal stress fields in a 6-inch silicon CZ system with a funnel-shaped radiation shield by finite element analysis based on the conduction-dominated model, and investigated theoretically the effect of radiation shield geometries on melt/crystal interface shape, crystal pull rate and thermal stresses in the crystal by comparing the present results with previous ones[15-17] for cylindrical and doughnut (torus)-shaped shields.

1. Theory

Figure 1 shows a schematic diagram of a silicon CZ puller with a funnel-shaped radiation shield inserted in the furnace. The details of the conduction-dominated model, and the finite element method for temperature and thermal stress distribution analysis used here, are found elsewhere[15,17].

The definitions of the dimensionless variables and dimensionless numbers are listed in the nomenclature. The calculated thermal stress field is expressed by the contour line of maximum shear stress defined by Eq. (1) for the sake of simplicity.

Received July 11, 1991. Correspondence concerning this article should be addressed to N. Imaishi.

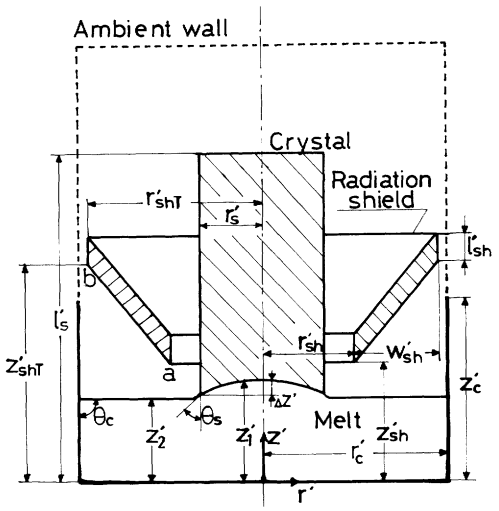

Fig. 1. Schematic diagram of CZ furnace with funnel-shaped radiation shield

$$\tau_{max}=(\tau_1-\tau_3)/2 \qquad (1)$$

where τ_1 and τ_3 are respectively the maximum and minimum values among the three local principal shear stresses.

The physical and mechanical properties used in the calculations are the same as those in the previous works[15,17], and the processing parameters are listed in **Table 1**. The shield is assumed to be made of graphite, unless its emissivity is specified.

2. Results and Discussion

Figure 2 shows the temperature profiles in the melt and crystal and the distributions of the maximum shear stresses. τ_{max}, in the crystal at different stages of crystal growth (*i.e.*, $V_m=0.23$ and 0.125). In the figure, (a) shows the results with a funnel-shaped radiation shield, (b) with a doughnut-shaped shield[16,17] and (c) without shield[16,17]. In all cases, the crystal radius and pull rate were kept constant ($r'_s=7.4$ cm, $Pe=0.1216$, which corresponds to a pull rate of 1 mm/min.), and thus the crucible temperature must be modulated as shown in Fig. 2. Compared with the results without a radiation shield, the funnel-shaped radiation shield makes the melt/crystal interface shape less convex to the crystal (relatively flatter), and also makes the thermal stresses in the crystal smaller, in a similar way to that with a doughnut-shaped shield[16,17].

We investigated the effects of the geometry, location and material properties of the funnel-shaped radiation shield on the heat transfer characteristics of the Si-CZ system, in order to determine the proper operating conditions of the CZ furnace with a shield.

Figure 3 shows the effect of the height of the funnel-shaped radiation shield, z_{sh}, on the maximum arc height (Δz) of the melt/crystal interface shown in

Table 1. Parameters used for calculations

Crucible radius	r'_c:	0.203 m
Crucible height	z'_c:	0.203 m
Crystal radius	r'_s:	0.074 m
Crystal length	l'_s:	0.183, 0.365, 0.629 m
Shield's bottom height	z'_{sh}:	0.071–0.173 m
Shield's bottom radius	r'_{sh}:	0.081–0.122 m
Shield's top height	z'_{shT}:	0.244 m
Sheild's top radius	r'_{shT}:	0.193 m
Sheild's depth	l'_{sh}:	0.003–0.030 m
Emissivity of shield	ε_{sh}:	0.10–0.68
Emissivity of graphite	ε:	$0.3789+(2.015E\text{-}4)\times T'$
Ambient wall temperature	T'_a:	673 K

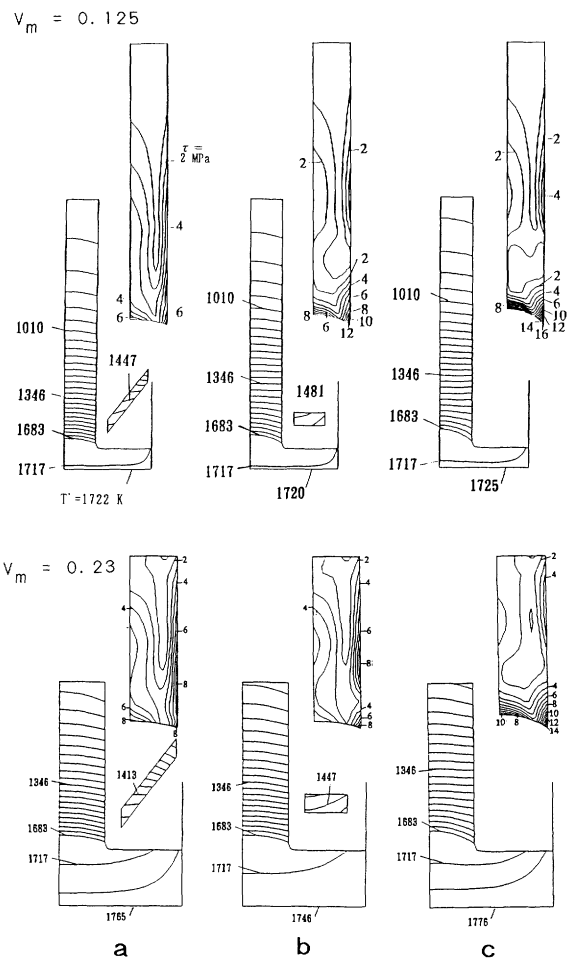

Fig. 2. Isotherms and iso-stress contours in CZ furnace with and without radiation shield at different melt volumes ($r'_s=7.4$ cm, $Pe=0.1216$)
(a) with a funnel-shaped shield; (b) with a doughnut-shaped shield; (c) without shield

Fig. 1, and on the crucible temperature, T_c. In Fig. 3, some of our previous results[15,16] are also plotted to investigate the effect of shield geometry. The calculated Δz with the funnel-shaped shield shows minimum value at some z_{sh}, and it is smaller than the minimum values for the other shield geometries, though a higher crucible temperature is required. **Figure 4** shows Δz as a function of the distance between

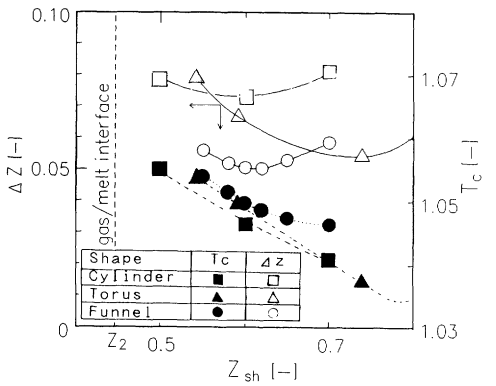

Fig. 3. Effect of z_{sh} on Δz and crucible temperature. ($V_m=0.23$, $Pe=0.1216$)
cylinder, $r_{sh}=0.6$, $l_{sh}=0.50$, $w_{sh}=0.02$; torus, $r_{sh}=0.5$, $l_{sh}=0.15$, $w_{sh}=0.35$; funnel, $r_{sh}=0.5$, $l_{sh}=0.15$, $w_{sh}=0.45$

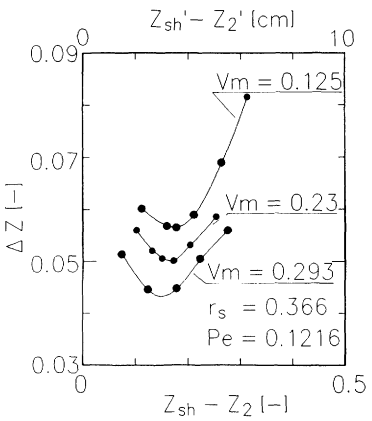

Fig. 4. Δz as a function of $(z_{sh}-z_2)$ at various melt volumes. ($l_{sh}=0.15$, $Pe=0.1216$)

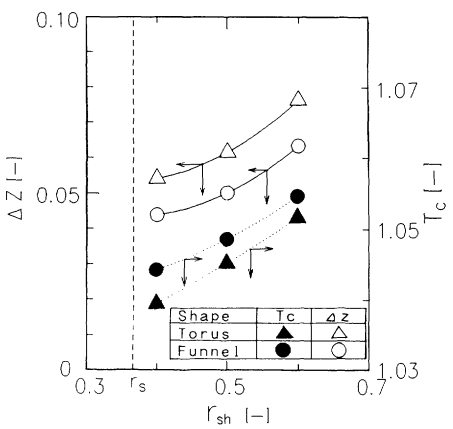

Fig. 5. Effect of bottom radius of shield on Δz and crucible temperature at $V_m=0.23$ and $Pe=0.1216$
torus, $l_{sh}=0.15$, $w_{sh}=0.35$, $z_{sh}=0.65$; funnel, $l_{sh}=0.15$, $r_{shT}=0.95$, $z_{sh}=0.62$

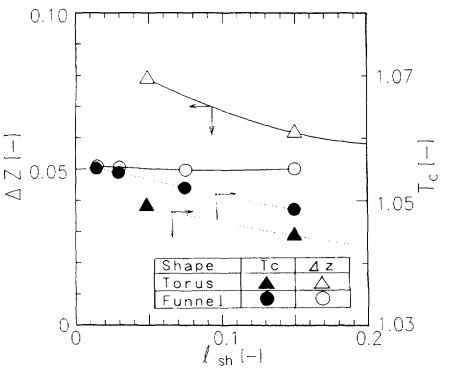

Fig. 6. Effect of shield thickness on Δz and crucible temperature at $V_m=0.23$, $r_{sh}=0.50$ and $Pe=0.1216$
torus, $z_{sh}=0.65$; funnel, $z_{sh}=0.62$

the melt surface and the bottom of the shield (see Fig. 1), $(z_{sh}-z_2)$, for three melt volumes.

It is found that Δz shows minimum value at some z_{sh}, and that the optimum position (corresponding to the smallest Δz) is approximately 3–4 cm above the melt surface for any melt volume. In the present industrial silicon CZ furnaces, the level of the melt surface is kept constant by lifting the crucible during crystal growth for the sake of diameter measurement and control via a fixed-focus ITV system. Then the radiation shield is not necessarily designed to be movable.

Figure 5 shows the effect of the bottom radius of the radiation shield on Δz and T_c for funnel- and doughnut-shaped shields. In both cases, Δz and T_c decrease as the shield approaches the radius of the crystal rod ($r_s=0.366$).

Figure 6 shows the effect of radiation shield thickness, l_{sh}, on Δz and T_c. For a doughnut-shaped radiation shield, Δz decreases as l_{sh} increases in the range shown in this figure. For a funnel-shaped shield, however, Δz does not depend on l_{sh}. The mechanism of Δz reduction by the doughtnut-shaped shield is thought to be that the shield reduces the radiative heat loss from the crystal bottom by reducing the view angle toward the cold ambient wall and thus reduces the radial temperature gradient there. Then the radiative heat loss and Δz depend largely on l_{sh}.

On the other hand, the funnel-shaped shield reduces Δz by reducing the net radiative heat loss by introducing radiative heat from the hot crucible to the crystal bottom. Thus l_{sh} is not a key factor on reducing Δz. But with the thinner shield, a higher crucible temperature is required to compensate the larger heat loss.

Figure 7 shows the changes in maximum arc height of the melt/crystal interface Δz and the required crucible temperature during constant-radius crystal growth with various pulling rates, where the radiation shield is located at its optimum position, *i.e.*, at z_{sh} corresponding to the smallest Δz for each melt volume. In Fig. 7, the dotted lines show the results without a radiation shield and with a doughnut-shaped one from the previous works[16]. Compared to these results, the funnel-shaped radiation shield provides a higher pull

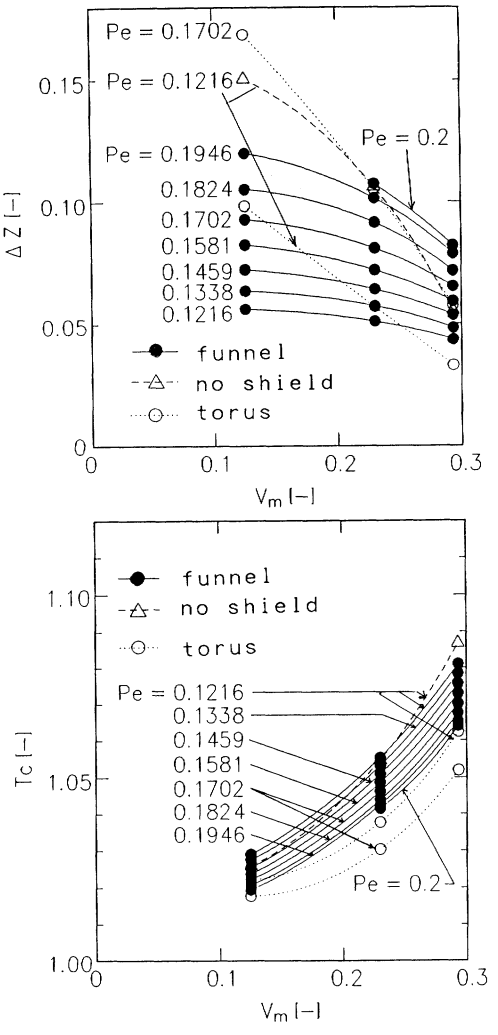

Fig. 7. Effects of pulling rate on Δz and crucible temperature for 6″ crystal growth. Each shield is located at optimum position
torus, $l_{sh}=0.15$, $w_{sh}=0.35$, $r_{sh}=0.50$; funnel, $l_{sh}=0.15$, $w_{sh}=0.45$, $r_{sh}=0.50$
The optimum z_{sh} at different V_m values are: at $V_m=0.293$, 0.23, 0.125; for torus shape, $z_{sh}=0.8$, 0.75, 0.5; for funnel shape, $z_{sh}=0.72$, 0.62, 0.42

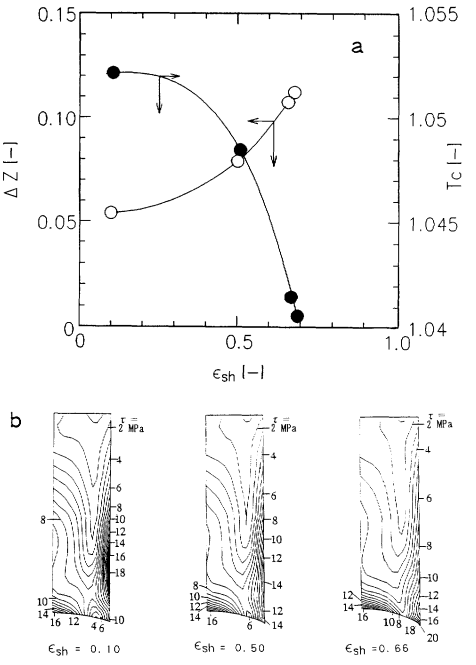

Fig. 8. Effect of emissivity of funnel-shaped shield, a) on Δz and crucible temperature, and b) on thermal stress distribution
($V_m=0.23$, $z_{sh}=0.62$, $l_{sh}=0.015$, $r_{sh}=0.50$, $Pe=0.20$)

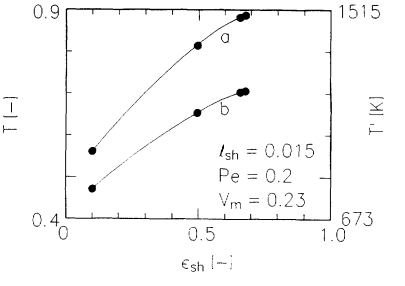

Fig. 9. Effect of emissivity of shield on temperaures at points **a** and **b** on the shield shown in Fig. 1. Conditions are given in Fig. 8

rate than do the others, if one allows a given value of Δz, or a flatter interface for a given pull rate, although a higher crucible temperature is required. In the initial period (when crystal is short and $V_m>0.25$), however, the CZ furnace with a funnel-shaped radiation shield gives a larger Δz than do the other furnaces. But Δz shows a less significant increase from top to bottom of the crystals.

Figure 8-a shows the effect of emissivity of the radiation shield on Δz and T_c. Apparently, the radiation shield with lower emissivity can make the melt/crystal interface less convex to the crystal (i.e., it reduces the thermal stress near the three-phase junction line as discussed in the previous paper[17]), while a higher temperature at the crucible wall is required to keep the crystal radius constant. Figure 8-b shows the thermal stress distributions in crystals growing in furnaces with funnel-shaped radiation shields of different emissivities. A funnel-shaped radiation shield made of material having smaller emissivity seems better for reducing thermal stress in the growing crystal. But a radiation shield with low emissivity is not acceptable from another point of view. **Figure 9** shows the temperatures at two points on the shield (points **a** and **b** in Fig. 1) as a function of the emissivity of the material. The temperature of the shield becomes remarkably low as the emissivity decreases. In practical operation of the CZ system, the surface temperature of any in-furnace structure must be high in order to prevent the precipitation of SiO which desorbs from the melt. **Figure 10** shows one example to realize small Δz with high shield temperature. In this case, a radiation shield made of

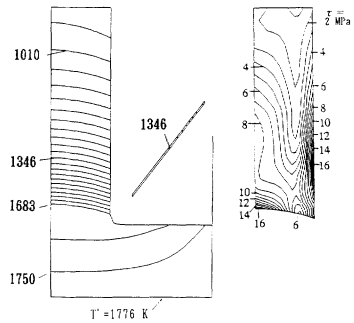

Fig. 10. Temperature and thermal stress distributions with a funnel-shaped shield made of graphite ($\varepsilon_{sh} \fallingdotseq 0.66$), whose two inner surfaces (facing the crystal) are assumed to be covered by a different material with $\varepsilon_{sh}=0.10$, ($V_m=0.23$, $z_{sh}=0.62$, $l_{sh}=0.015$, $r_{sh}=0.50$, $Pe=0.20$)

graphite ($\varepsilon \fallingdotseq 0.66$) is assumed to be covered with a different material ($\varepsilon=0.1$) on its two sides facing the crystal. From Fig. 10 it is found that modulation of the material property can increase the temperature at the shield surface (T at points a and b 0.810 and 0.657 respectively) and at the same time decrease Δz ($\Delta z=0.0666$ at $T_c=1.0553$) and thermal stresses.

The conventional (without radiation shield) CZ furnace must be operated in rather narrowly restricted conditions, because of the simple structures and the strong thermal coupling between them. But our work indicates that the appropriate choice of radiation shield (shape and material) can greatly expand the operating conditions of the silicon CZ system.

Conclusion

Analyses of temperature and thermal stress fields and of the shape of the melt/crystal interface in 6″ silican crystal growth with a funnel-shaped radiation shield were carried out, using the finite element method. The following points were revealed.

(1) The funnel-shaped radiation shield is sufficiently effective to flatten the melt/crystal interface, to increase the pulling rate and also to reduce thermal stresses in the crystal by setting the shield in the optimum location, in addition to control of the gas flow in the CZ furnace.

(2) Choice of emissivity and geometry of the radiation shield can widely change the operating conditions of a CZ system.

Nomenclature

C_p	=	specific heat	[J/kg/K]
H_f	=	latent heat of fusion	[J/kg]
k	=	thermal conductivity	[W/m/K]
l'_s	=	crystal length	[m]
l'_{sh}	=	thickness of radiation shield	[m]
l_s, l_{sh}	=	l'_s/r'_c, l'_{sh}/r'_c	[—]
Pe	=	Peclet number ($=\rho_s C_{ps} V'_s r'_c/k_l$)	[—]
r'	=	radial distance in cylindrical coordinates	[m]
r'_c	=	crucible radius	[m]
r'_s	=	crystal radius	[m]
r'_{sh}	=	radiation shield radius	[m]
r, r_s, r_{sh}	=	r'/r'_c, r'_s/r'_c, r'_{sh}/r'_c	[—]
St	=	Stefan number ($=H_f/C_{ps}T'_m$)	[—]
T'	=	temperature	[K]
T'_a	=	ambient temperature	[K]
T'_c	=	crucible temperature	[K]
T'_m	=	melting point temperature	[K]
T, T_c	=	T'/T'_m, T'_c/T'_m	[—]
V'_m	=	melt volume	[m^3]
V_m	=	$V'_m/2\pi r'^3_c$	[—]
V'_s	=	crystal pull rate	[m/s]
w'_{sh}	=	radiation shield width	[m]
w_{sh}	=	w'_{sh}/r'_c	[—]
z'	=	axial distance in cylindrical coordinates	[m]
z'_c	=	crucible height	[m]
z'_2	=	melt depth	[m]
z'_{sh}	=	radiation sheild height	[m]
$\Delta z'$	=	maximum arc height of melt/crystal interface	[m]
z, z_c, z_2	=	z'/r'_c, z'_c/r'_c, z'_2/r'_c	[—]
z_{sh}, Δz	=	z'_{sh}/r'_c, $\Delta z'/r'_c$	[—]
ε	=	emissivity	[—]
θ_c, θ_s	=	contact angle	[deg.]
κ	=	k_s/k_l	[—]
ν	=	Poisson's ratio	[—]
ρ	=	density	[kg/m^3]
σ	=	Stefan-Boltzman constant	[W/m^3/K]
τ_{max}	=	maximum shear stress	[Pa]
τ_1, τ_3	=	local principle shear stress	[Pa]

〈Subscript〉

l	=	melt
s	=	crystal
sh	=	radiation shield
shT	=	at top of shield

Literature Cited

1) Bornside, D. E., T. A. Kinney and R. A. Brown: *J. Crystal Growth*, **108**, 779 (1991).
2) Chan, Y. T., H. J. Gibeling and H. L. Grubin: *J. Appl. Phys.*, **64**, 1425 (1988).
3) Crowley, A. B., E. J. Stern and D. T. J. Hurle: *J. Crystal Growth*, **97**, 697 (1989).
4) Derby, J. J. and R. A. Brown: *J. Crystal Growth*, **83**, 137 (1987).
5) Derby, J. J. and R. A. Brown: *J. Crystal Growth*, **87**, 251 (1988).
6) Derby, J. J., L. J. Atherton and P. M. Gresho: *J. Crystal Growth*, **97**, 792 (1989).
7) Dupret, F., P. Nicodeme and Y. Ryckmans: *J. Crystal Growth*, **97**, 162 (1989).
8) Ishida, M., K. Katano, S. Kawabata, Y. Higuchi, F. Orito, Y. Yamaguchi, F. Yajima and T. Okano: *J. Crystal Growth*, **99**, 707 (1990).
9) Kopetsch, H.: *J. Crystal Growth*, **88**, 71 (1988).
10) Kopetsch, H.: *J. Crystal Growth*, **102**, 505 (1990).
11) Meduoye, G. O., K. E. Evans and D. J. Bacon: *J. Crystal Growth*, **97**, 709 (1989).
12) Miyahara, S., S. Kobayashi, T. Fujiwara, T. Kubo and H. Fujiwara: *J. Crystal Growth*, **99**, 696 (1990).
13) Motakef, S.: *J. Crystal Growth*, **88**, 341 (1988).
14) Motakef, S.: *J. Crystal Growth*, **96**, 201 (1989).
15) Tsukada, T., N. Imaishi, M. Hozawa and —. Fujinawa: *J. Chem. Eng. Japan*, **20**, 146 (1987).

16) Tsukada, T., N. Imaishi and M. Hozawa: *J. Chem. Eng. Japan*, **21**, 381 (1988).
17) Tsukada, T., M. Hozawa and N. Imaishi: *J. Chem. Eng. Japan*, **23**, 186 (1990).
18) Virzi, A.: *J. Crystal Growth*, **97**, 152 (1989).